


Two Phases Inside the Bose Condensation Dome of $\text{Yb}_2\text{Si}_2\text{O}_7$

Michael O. Flynn^{1,*}, Thomas E. Baker², Siddharth Jindal,³ and Rajiv R. P. Singh¹

¹*Department of Physics, University of California, Davis, Davis, California 95616, USA*

²*Institut quantique & Département de physique, Université de Sherbrooke, Sherbrooke, Québec J1K 2R1 Canada*

³*Department of Physics, University of Illinois at Urbana-Champaign, Urbana, Illinois 61801, USA*

 (Received 23 January 2020; revised 5 December 2020; accepted 15 January 2021; published 12 February 2021)

Recent experimental data on Bose-Einstein condensation of magnons in the spin-gap compound $\text{Yb}_2\text{Si}_2\text{O}_7$ revealed an asymmetric Bose-Einstein condensation dome [G. Hester et al., *Phys. Rev. Lett.* **123**, 027201 (2019)]. We examine modifications to the Heisenberg model on a breathing honeycomb lattice, showing that this physics can be explained by competing anisotropic perturbations. We employ a gamut of analytical and numerical techniques to show that the anisotropy yields a field driven phase transition from a state with broken Ising symmetry to a phase that breaks no symmetries and crosses over to the polarized limit.

DOI: [10.1103/PhysRevLett.126.067201](https://doi.org/10.1103/PhysRevLett.126.067201)

In recent decades, models of localized spins have been shown to contain a wealth of familiar and exotic phases of matter. Interesting orders can be achieved by considering models with competing interactions, which naively require the satisfaction of incompatible constraints to achieve a ground state. Nature's creative mechanisms for resolving these tensions within quantum mechanics are responsible for much of the diversity of phenomena observed within many-body theory [1–7].

A clear example of such physics is found in dimer magnetism, where antiferromagnetic behavior is brought into tension with polarizing magnetic fields [8–13]. In these systems, spins tend to pair into singlets in the low-field ground state. A simple example of this phenomenon is realized in the antiferromagnetic Heisenberg model on the breathing honeycomb lattice. As illustrated in Fig. 1(a), each spin has a preferred neighbor due to lattice distortion that picks out pairs of spins that dimerize in the ground state.

Applying a magnetic field to the singlet state generically leads to a Bose-Einstein condensation (BEC) transition where a triplet band becomes degenerate with the $S = 0$ ground state, creating a planar antiferromagnet. In typical experiments [9], it has been found that strengthening this field eventually polarizes the system; no other phase transitions are observed. Recently, experiments on the compound $\text{Yb}_2\text{Si}_2\text{O}_7$ have challenged this paradigm by suggesting the presence of an intermediate magnetic phase with an unknown underlying order [8]. This Letter proposes a modification to the Heisenberg model whose ground state order is consistent with all available thermodynamic data and allows for the possibility of such a phase diagram.

On the breathing honeycomb lattice, the Heisenberg model in a magnetic field only realizes the previously mentioned singlet, XY antiferromagnet, and polarized phases. In order to model the additional phase observed

experimentally, we generalize the Heisenberg model by introducing two forms of anisotropy:

$$H = \sum_{\langle ij \rangle, \alpha} J_{ij}^{\alpha} S_i^{\alpha} S_j^{\alpha} - h \sum_{i \in A, \alpha} g_{z\alpha}^A S_i^{\alpha} - h \sum_{j \in B, \alpha} g_{z\alpha}^B S_j^{\alpha}. \quad (1)$$

Here i, j index lattice sites, A, B are sublattices, and $\alpha = x, y, z$. The x, y, z directions correspond, respectively,

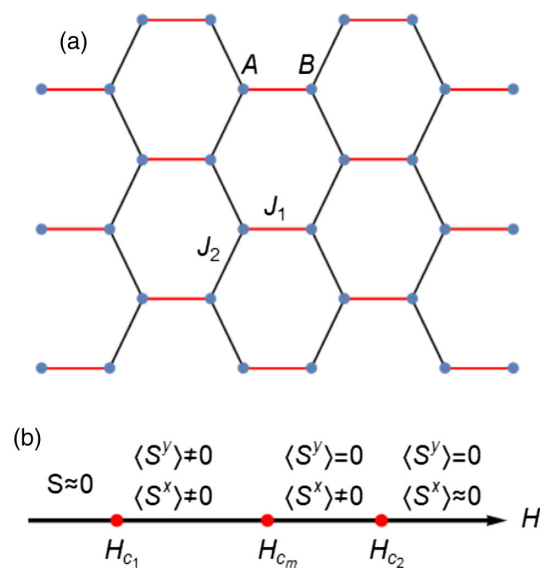


FIG. 1. Honeycomb lattice model and $T = 0$ phase diagram. (a) A section of the honeycomb lattice. Each spin (blue dots) has a preferred neighbor (red bonds) which it interacts with more strongly than others: $J_1 > J_2$. For $h = 0$, the ground state is a product of singlets along the red bonds. (b) Schematic $T = 0$ phase diagram obtained from DMRG and mean-field theory. From left to right, the phases are a global spin singlet, \mathbb{Z}_2 symmetry breaking antiferromagnet, canted antiferromagnet, and the polarized phase. The critical points H_{c_1} and H_{c_m} are in the Ising universality class while H_{c_2} is a crossover.

to the a^* , $b = b^*$, and c axes of the C2/m lattice structure. The sublattice dependence of the g tensor allows for a staggered component $g_{zx}^A = -g_{zx}^B$, which is essential to the universal physics we will describe. The “minimal model” for the physics of interest is significantly simpler: it is sufficient to take $J_{ij}^y > J_{ij}^x = J_{ij}^z$ (for all i, j) and $g_{zy} = 0$, as y is a principal axis. The more precise constraints discussed below are imposed by consistency with experiments.

As we will see, there is a regime of parameters that yields the phase diagram in Fig. 1(b). This phase diagram matches thermodynamic data by providing a mechanism for breaking and restoring an Ising symmetry as an external magnetic field is tuned. For $H_{c_1} < H < H_m$, the ground state breaks a \mathbb{Z}_2 symmetry in spin space associated with the global transformation $S_i^y \rightarrow -S_i^y$, while for $H > H_m$ the system exhibits no symmetry breaking. Importantly, these effects are observable with weak anisotropy: we believe this can explain the coexistence of the familiar and unfamiliar features observed in $\text{Yb}_2\text{Si}_2\text{O}_7$ [8].

We will use a variety of complementary techniques to develop a theory that accounts for the observations of $\text{Yb}_2\text{Si}_2\text{O}_7$. In order to motivate our model, Eq. (1), we begin with a review of salient experimental facts. We then use a linked cluster expansion to compute the triplon spectrum and critical fields of the pure Heisenberg model, H_{c_1} and H_{c_2} . Our results are consistent with experimental findings and confirm that the Heisenberg model captures important aspects of the physics of $\text{Yb}_2\text{Si}_2\text{O}_7$. Spin-wave theory is then applied to the full Eq. (1) Hamiltonian to show that the perturbations we have introduced produce dispersion relations that are qualitatively consistent with neutron scattering data. We then develop an understanding of the new order induced by these perturbations through a self-consistent mean-field theory, which reveals the previously undetermined ground state order to be a canted antiferromagnet with a large staggered magnetic susceptibility. This physical picture is then quantitatively verified via a density matrix renormalization group (DMRG) analysis, and our concluding remarks suggest experimental tests of our proposal.

Experimental considerations.—Plausible modifications to the Heisenberg model are strongly constrained by the available experimental data. To establish constraints on the parameters introduced in Eq. (1), we review the salient experimental results [8]. (1) *Critical fields and zero-field specific heat are modeled well by the pure Heisenberg model.* In Ref. [8], it was demonstrated that the Heisenberg model fits zero-field specific heat data. We will also show that the Heisenberg model is consistent with the empirical values of H_{c_1} and H_{c_2} . (2) *The XY antiferromagnet hosts an approximate Goldstone mode.* Within the energy resolution of available data, there is a gapless mode in the band structure of the planar antiferromagnet. (3) *Singularities in the specific heat present in weak fields vanish with increasing field.* In weak fields, an Ising-like singularity is observed as a function of temperature. Increasing the

field to $H_m \approx 1.2$ T removes the singularity and leads to smooth behavior as a function of temperature. Ultrasound velocity and neutron scattering measurements offer additional evidence of a phase transition at H_m .

Together, these points suggest that the Heisenberg model provides a strong basis for an analysis of $\text{Yb}_2\text{Si}_2\text{O}_7$. However, it is clear that the ground state breaks different (discrete) symmetries as a function of the magnetic field, which is not a feature of the pure Heisenberg model. Moreover, the ground state for $H > H_m$ smoothly crosses over to the polarized limit at $H = H_{c_2}$.

Phenomenology of the model.—The perturbations to the Heisenberg model that we have introduced are designed to respect these experimental constraints, while providing a mechanism for breaking and restoring an Ising symmetry as a magnetic field is applied. The key changes are to the XY Heisenberg couplings, $J_{ij}^y = (1 + \lambda)J_{ij}^x$ and a staggered g -tensor component $g_{zx} \ll g_{zz}$, $g_{zx}^A = -g_{zx}^B$. By choosing $\lambda \ll 1$, the first two experimental points are addressed: many qualitative features of the Heisenberg model are preserved and the Goldstone mode is only weakly gapped. The staggered g tensor creates a field-dependent competition between antiferromagnetic orders in the X-Y plane. In weak magnetic fields ($H_{c_1} < H < H_m$), the YY coupling dominates, and the ground state breaks the \mathbb{Z}_2 spin symmetry of the Hamiltonian. In larger magnetic fields ($H > H_m$), no symmetry is broken because the staggered g tensor selects a unique antiferromagnetic order. Since it breaks no symmetries, this state can cross over smoothly to the polarized limit ($H > H_{c_2}$).

We note that a staggered g tensor is forbidden by the inversion symmetry of the C2/m crystal structure. However, weak deviations from this structure due to lattice distortions are not ruled out by available data. Such a distortion has clear experimental signatures (see the concluding section). The required weakness of our staggered g tensor (see Fig. 5 and surrounding discussions) is consistent with a distortion-based explanation.

Furthermore, we have explored similar models with uniform g tensors and found that they do not reproduce the phase diagram of Fig. 1. Essentially, a uniform g tensor does not lead to a field-dependent competition between antiferromagnetic orders: instead, spins simply have a polarization in the X-Z plane proportional to the effective field in each direction. While we have not completely ruled out the possibility that a model with inversion symmetry could produce the correct universal physics, we believe that no such model is consistent with the aforementioned experimental constraints.

The parameters we will choose throughout this Letter, unless otherwise noted, are $\lambda = 0.03$ and $g_{zx} = g_{zz}/100$. We take the x component of the Heisenberg coupling to be the value obtained experimentally for the isotropic Heisenberg model, $J_1^x = 0.2173$ meV, $J_2^x = 0.0891$ meV. Conversions to physical magnetic fields are done with g

factors measured in [8]. We have found that our results do not qualitatively depend on these choices except in our DMRG analysis, where this issue is discussed.

Linked-cluster expansion.—Here we simplify to the isotropic Heisenberg model ($\lambda = 0$) and assume the z axis is a principal axis of g ($g_{z\alpha} \propto \delta_{z\alpha}$). We will perturbatively compute the critical fields of the BEC transition and show that the result is consistent with experiments. In the limit $J_2 = h = 0$, the ground state of Eq. (1) is a collection of independent spin singlets. For finite J_2 with $J_2/J_1 \ll 1$, the ground state remains in the $S = 0$ sector with a gap to mobile triplet excitations. We compute the spectrum of these “single-particle” states with the linked-cluster formalism. This yields a perturbative expression in J_2/J_1 that accurately describes the thermodynamic limit [14–16].

The resulting spectrum has a minimum at $\mathbf{k} = 0$, and we find that (defining $J_2/J_1 = \alpha$)

$$\omega(\mathbf{k} = 0) = J_1 \left[1 - \alpha - \alpha^2 + \frac{5}{16} \alpha^3 + \mathcal{O}(\alpha^4) \right]. \quad (2)$$

For $h \neq 0$, the $S^z = 1$ triplet band decreases linearly in energy leading to a gap closing. The resulting BEC transition has been studied extensively [9,17–22]. Choosing the couplings and gyromagnetic factors reported in Ref. [8], we find the critical field $H_{c_1} \approx 0.434$ T, in rough agreement with the experimental data. The upper critical field, H_{c_2} , of the Heisenberg model can be calculated exactly by considering the energetic cost of a spin flip in the polarized phase. We find $H_{c_2} = J_1 + 2J_2 \approx 1.42$ T, also in agreement with experiment.

The singlet ansatz for the ground state is not correct in the presence of anisotropy when $h \neq 0$. However both mean-field and DMRG analyses indicate that the system becomes effectively paramagnetic below H_{c_1} in the presence of weak anisotropy (see Fig. 4). The agreement between these critical fields and the experimental results provides an *a posteriori* justification for our focus on perturbative adjustments to the Heisenberg model.

Spin-wave theory.—By introducing anisotropy to the Heisenberg couplings, we have broken the XY symmetry of the model. We therefore anticipate that the spectrum is gapped, and the Goldstone mode observed experimentally is in fact massive. Here we will use linear spin-wave theory to compute the spectrum and show that the resulting bands are qualitatively consistent with neutron scattering data. (Additional details of spin-wave theory are available in the Supplemental Material [23].)

Our ansatz for the classical spin orientations on sublattices A, B is for a canted antiferromagnet:

$$\begin{aligned} \mathbf{S}_A &= S(\sin \theta \cos \phi, \sin \theta \sin \phi, \cos \theta) \\ \mathbf{S}_B &= S(-\sin \theta \cos \phi, -\sin \theta \sin \phi, \cos \theta). \end{aligned} \quad (3)$$

Minimizing the Hamiltonian as a function of θ, ϕ yields two solutions. In weak fields,

$$\begin{aligned} \cos \theta &= \frac{h_z}{S(\bar{J}_z + \bar{J}_y)} \\ \cos \phi &= \frac{h_x(\bar{J}_z + \bar{J}_y)}{(\bar{J}_y - \bar{J}_x) \sqrt{S^2(\bar{J}_z + \bar{J}_y)^2 - h_z^2}}. \end{aligned} \quad (4)$$

Here $\bar{J}_\alpha = J_1^\alpha + 2J_2^\alpha$, $h_z = g_{zz}h$, $h_x = g_{zx}h$. The critical field $H_m \approx 1.2$ T is given by the condition $\cos \phi = 1$ and agrees with experimental data. For $H > H_m$, the system transitions to the solution

$$\begin{aligned} \phi &= 0 \\ \sin \theta &= \frac{h_z \tan \theta - h_x}{S(\bar{J}_z + \bar{J}_x)}. \end{aligned} \quad (5)$$

Using the Holstein-Primakoff mapping to bosons, we obtain a quadratic Hamiltonian that can be diagonalized using standard techniques [24–26]. From the resulting dispersion, we extract the band gap as a function of the magnetic field (Fig. 2). The bands are gapped everywhere except at H_m , which separates the spin-wave solutions. The value of the gap exceeds experimental results; however, key qualitative details that we expect are universal are captured [23].

Cluster mean-field theory.—In order to describe the novel phase observed in $\text{Yb}_2\text{Si}_2\text{O}_7$, we move on to develop a qualitative understanding of the ground states of Eq. (1). We begin by formulating a mean-field theory using the bipartite structure of the honeycomb lattice. Let $\mathbf{M}_A, \mathbf{M}_B$ denote the average magnetic moments on sublattices A, B . The enhanced coupling J_1 between neighbors along $y = b$ suggests that the fundamental degree of freedom is a dimer containing spins $\mathbf{S}_A, \mathbf{S}_B$ embedded in an effective field. The Hamiltonian is

$$\begin{aligned} H &= J_1^\alpha S_A^\alpha S_B^\alpha + 2J_2^\alpha (S_A^\alpha M_B^\alpha + S_B^\alpha M_A^\alpha) \\ &\quad - h \sum_\alpha (g_{z\alpha}^A S_A^\alpha + g_{z\alpha}^B S_B^\alpha). \end{aligned} \quad (6)$$

We assume $g_{zx} \ll g_{zz}$. The Eq. (6) Hamiltonian is analyzed with self-consistent methods, starting with an

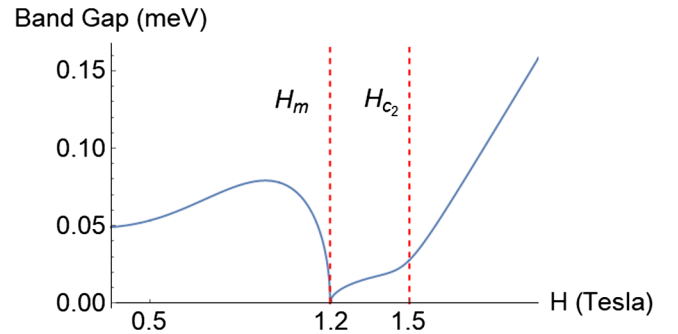


FIG. 2. Band gap as a function of field in linear spin-wave theory. Other than the phase transition between spin-wave solutions at $H = H_m$ (see text), the system is gapped with an energy scale near the energy resolution of available neutron scattering data. For $H > H_{c_2}$ the band gap scales linearly with H .

ansatz for $\mathbf{M}_A, \mathbf{M}_B$ and calculating new values $\mathbf{M}_i \equiv \langle \psi | \mathbf{S}_i | \psi \rangle$, where $|\psi\rangle$ is the instantaneous ground state. These values are updated until convergence is achieved.

For sufficiently small g_{zx} , we find that the solution in Fig. 3 is energetically favored. For small fields ($H < H_{c_1}$), the solution is weakly magnetic due to the staggered field induced by g_{zx} . Between the critical fields $H_{c_1} < H < H_{c_2}$, two phases appear, distinguished by the staggered moment M_y . The first ($H < H_m$) exhibits \mathbb{Z}_2 symmetry breaking and accounts for the singularity observed in the specific heat; the latter breaks no symmetries and crosses over smoothly to the polarized limit, as required by the absence of thermodynamic singularities. This previously unidentified phase is a canted antiferromagnet.

We note the existence of another mean-field solution in which $M_y = 0$ everywhere. This case does not support the experimental data as it has no symmetry breaking. The energetic favorability of one solution over another depends on the precise anisotropy parameters chosen; it is unclear how quantum fluctuations will impact that selection. Furthermore, it is not obvious that the interdimer coupling J_2 is sufficiently small to justify a mean-field description. To address these concerns, we employ DMRG to investigate the stability of our results. There we find that both mean-field solutions survive quantum fluctuations and remain energetically competitive. Furthermore, there is a regime of parameters in which the solution in Fig. 3 is favored. Additional mean-field data is available in the Supplemental Material [23].

DMRG analysis.—To verify the mean-field solution, we use DMRG to compute ground state expectation values [27]. This tensor network method efficiently simulates systems that are well described by the matrix product state

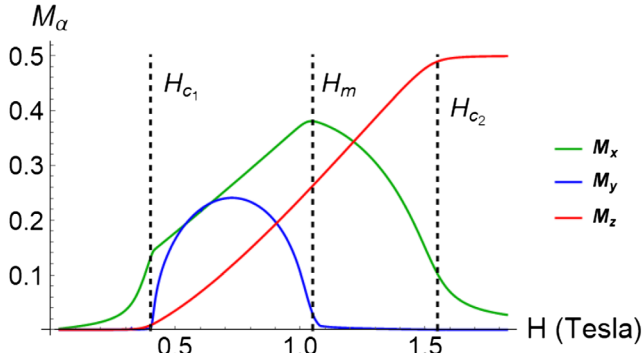


FIG. 3. Spin expectation values as a function of magnetic field obtained from mean-field theory ($\lambda = 0.03$, $g_{zx} = g_{zz}/100$). Note that the X and Y moments are staggered, while Z is uniform. The presence of a nonzero M_y for $H_{c_1} < H < H_m$ indicates \mathbb{Z}_2 symmetry breaking and corresponds to the standard magnetic phase observed on the high-field side of the BEC phase transition without anisotropy. The range $H_m < H < H_{c_2}$ corresponds to a canted antiferromagnet that breaks no symmetries and crosses over to the saturated regime at H_{c_2} .

ansatz [28–32]. Our system is studied on a cylinder with a width of four dimers and 128 total spins.

We use a single-site representation of the renormalized tensor network to update each step [33] with the Eq. (1) Hamiltonian. To guarantee that the proper symmetry sector is obtained, we apply pinning fields on the open boundaries of the system to break the \mathbb{Z}_2 symmetry of the Hamiltonian. The pinning field is removed after two DMRG sweeps, and we find that in the symmetry-breaking region this produces a lower-energy state than an unbiased DMRG.

From the resulting ground-state wave function, local measurements of quantities $M_\alpha = \sqrt{\sum_{i=1}^{N_s} \langle \hat{S}_i^\alpha \rangle^2} / N_s$ are performed. The results are shown in Fig. 4 and qualitatively match those from mean-field theory. The nonzero value of M_y for $H_{c_1} < H < H_m$ requires \mathbb{Z}_2 symmetry breaking. This symmetry is restored for $H > H_m$, allowing for a smooth crossover to the polarized limit at H_{c_2} . The regime $H_m < H < H_{c_2}$ is distinguished from the polarized limit by the large staggered susceptibility of X moments and the continued growth of the Z magnetization. Similar methods allow for direct comparison to ultrasound velocity data (see the Supplemental Material [23]).

The results in Fig. 4 are found with $g_{xz} = g_{zz}/500$. This value is arbitrary and can affect which mean-field solution is obtained; to account for this, Fig. 5 shows the dependence of the symmetry-breaking order parameter M_y on g_{zx} in a fixed magnetic field. The solutions were found by first tuning to $H = 0.9$ T with pinning fields. The pinning fields are then removed, and g_{zx} is increased. The ground state changes from a Y-ordered antiferromagnet to a state where $M_y = 0$ as g_{zx} increases. The instability of the symmetry-breaking solution to anisotropy in the g tensor reveals that g_{zx} is necessarily small. This is consistent with the fact that a nonzero g_{zx} requires deviations from the C2/m crystal structure currently proposed experimentally; such

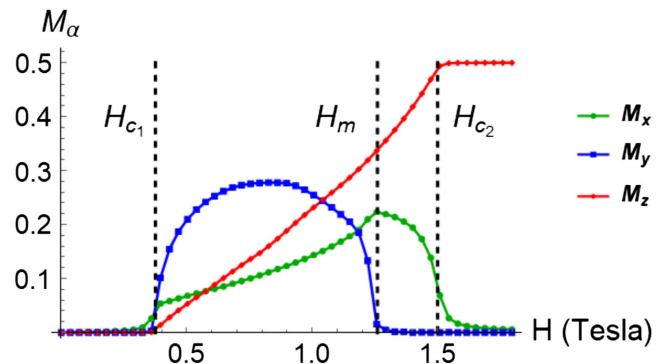


FIG. 4. Spin expectation values as a function of magnetic field from DMRG ($\lambda = 0.03$, $g_{zx} = g_{zz}/500$). The qualitative agreement with Fig. 3 confirms that the universal physics obtained via mean-field theory is accurate. The data again indicate a field-driven phase transition from a broken symmetry state ($H_{c_1} < H < H_m$) to a state that breaks no symmetries ($H_m < H < H_{c_2}$).

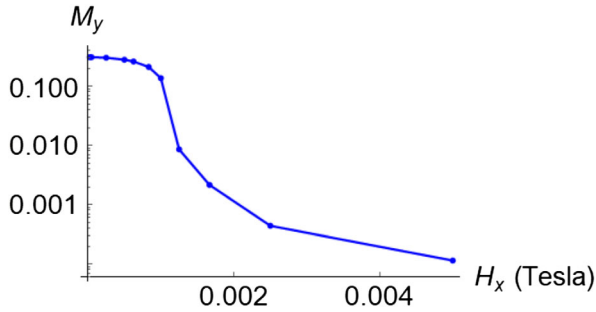


FIG. 5. Dependence of M_y on the magnitude of the staggered field $H_x = g_{zx}H$ ($H = 0.9$ T for each point). The value of M_y drops off rapidly with g_{zx} , indicating an instability of the symmetry-breaking mean-field solution to anisotropy in the g tensor. Weakness of the anisotropy is therefore critical to the physics.

distortions are expected to be weak. The qualitative features of the phase diagram should be robust to other perturbations.

Conclusions.—With a variety of theoretical techniques, we have constructed an explanation for the experimentally proposed phase diagram of $\text{Yb}_2\text{Si}_2\text{O}_7$. These techniques complement each other; each of them supports the physical picture presented in this Letter. We emphasize again that weak perturbations to the Heisenberg model can explain the observed thermodynamic responses of the material, with an associated reduction of crystallographic symmetry.

Experimental verification of these details remains crucial, and our theory suggests natural tests of itself. The structure of local magnetic moments in the material can be probed with nuclear magnetic resonance techniques. In particular, observation of a staggered magnetization along a^* in the regime $H_m < H < H_{c_2}$ would confirm that a $C2/m$ forbidden, staggered g tensor is crucial to describing $\text{Yb}_2\text{Si}_2\text{O}_7$. Furthermore, more precise neutron scattering measurements may reveal a spin gap for $H_{c_1} < H < H_m$, the magnitude of which will constrain the XY anisotropy of our model.

We thank Leon Balents and Frédéric Mila for suggestions in the development of the mean-field theory. We are also grateful to Miles Stoudenmire for helpful comments on DMRG techniques. We acknowledge useful discussions with Kate Ross and Jeffrey Quilliam. We thank the Institute for Complex Adaptive Matter (ICAM)-supported school on Emergent Phenomena in Correlated Quantum Matter in Cargèse, where this collaboration was initiated. The work of M. F. and R. R. P. S. is supported in part by NSF DMR Grant No. 1855111. The work of S. J. is supported in part by NSF PHY Grant No. 1852581. T. E. B. acknowledges the support of the Postdoctoral Fellowship from Institut Quantique and support from Institut Transdisciplinaire d'Information Quantique (INTRIQ). This research was undertaken thanks in part to funding from the Canada First Research Excellence Fund (CFREF). This research

was enabled in part by support provided by Calcul Québec [34] and Compute Canada [35]. Computations were made on the supercomputer Mammouth (mp2) located at Université de Sherbrooke.

*Corresponding author.
miflynn@ucdavis.edu

- [1] L. Savary and L. Balents, *Rep. Prog. Phys.* **80**, 016502 (2017).
- [2] M. J. P. Gingras and P. A. McClarty, *Rep. Prog. Phys.* **77**, 056501 (2014).
- [3] F.-Y. Li, Y.-D. Li, Y. B. Kim, L. Balents, Y. Yu, and G. Chen, *Nat. Commun.* **7**, 12691 (2016).
- [4] L. Balents, *Nature (London)* **464**, 199 (2010).
- [5] J. B. Kogut, *Rev. Mod. Phys.* **51**, 659 (1979).
- [6] A. Ortiz-Ambriz, C. Nisoli, C. Reichardt, C. J. O. Reichardt, and P. Tierno, *Rev. Mod. Phys.* **91**, 041003 (2019).
- [7] E. Fradkin, *Field Theories of Condensed Matter Physics*, 2nd ed. (Cambridge University Press, Cambridge, England, 2013).
- [8] G. Hester, H. S. Nair, T. Reeder, D. R. Yahne, T. N. DeLazzer, L. Berges, D. Ziat, J. R. Neilson, A. A. Aczel, G. Sala, J. A. Quilliam, and K. A. Ross, *Phys. Rev. Lett.* **123**, 027201 (2019).
- [9] V. Zapf, M. Jaime, and C. D. Batista, *Rev. Mod. Phys.* **86**, 563 (2014).
- [10] V. S. Zapf, D. Zocco, B. R. Hansen, M. Jaime, N. Harrison, C. D. Batista, M. Kenzelmann, C. Niedermayer, A. Lacerda, and A. Paduan-Filho, *Phys. Rev. Lett.* **96**, 077204 (2006).
- [11] M. Kofu, H. Ueda, H. Nojiri, Y. Oshima, T. Zenmoto, K. C. Rule, S. Gerischer, B. Lake, C. D. Batista, Y. Ueda *et al.*, *Phys. Rev. Lett.* **102**, 177204 (2009).
- [12] Y. Tsui, A. Brühl, K. Removic-Langer, V. Pashchenko, B. Wolf, G. Donath, A. Pikul, T. Kretz, H.-W. Lerner, M. Wagner, A. Salguero, T. Saha-Dasgupta, B. Rahaman, R. Valentí, and M. Lang, *J. Magn. Magn. Mater.* **310**, 1319 (2007).
- [13] U. Tutsch, B. Wolf, S. Wessel, L. Postulka, Y. Tsui, H. Jeschke, I. Opahle, T. Saha-Dasgupta, R. Valentí, A. Brühl, K. Remović-Langer, T. Kretz, H.-W. Lerner, M. Wagner, and M. Lang, *Nat. Commun.* **5**, 5169 (2014).
- [14] M. P. Gelfand, R. R. P. Singh, and D. A. Huse, *J. Stat. Phys.* **59**, 1093 (1990).
- [15] M. P. Gelfand and R. R. P. Singh, *Adv. Phys.* **49**, 93 (2000).
- [16] J. Oitmaa, C. Hamer, and W. Zheng, *Series Expansion Methods for Strongly Interacting Lattice Models* (Cambridge University Press, Cambridge, England, 2006).
- [17] C. D. Batista and G. Ortiz, *Phys. Rev. Lett.* **86**, 1082 (2001).
- [18] H. Tanaka, F. Yamada, T. Ono, T. Sakakibara, Y. Uwatoko, A. Oosawa, K. Kakurai, and K. Goto, *J. Magn. Magn. Mater.* **310**, 1343 (2007).
- [19] D. S. Fisher and P. C. Hohenberg, *Phys. Rev. B* **37**, 4936 (1988).
- [20] E. Orignac, R. Citro, and T. Giamarchi, *Phys. Rev. B* **75**, 140403(R) (2007).
- [21] O. Nohadani, S. Wessel, B. Normand, and S. Haas, *Phys. Rev. B* **69**, 220402(R) (2004).

- [22] T. Giamarchi, C. Rüegg, and O. Tchernyshyov, *Nat. Phys.* **4**, 198 (2008).
- [23] See Supplemental Material at <http://link.aps.org/supplemental/10.1103/PhysRevLett.126.067201> for additional data from spin-wave theory, mean-field theory, and DMRG.
- [24] T. Holstein and H. Primakoff, *Phys. Rev.* **58**, 1098 (1940).
- [25] M. Mourigal, W. T. Fuhrman, A. L. Chernyshev, and M. E. Zhitomirsky, *Phys. Rev. B* **88**, 094407 (2013).
- [26] M. E. Zhitomirsky and A. L. Chernyshev, *Rev. Mod. Phys.* **85**, 219 (2013).
- [27] S. R. White, *Phys. Rev. Lett.* **69**, 2863 (1992).
- [28] T. E. Baker, S. Desrosiers, M. Tremblay, and M. P. Thompson, [arXiv:1911.11566](https://arxiv.org/abs/1911.11566).
- [29] I. Affleck, T. Kennedy, E. H. Lieb, and H. Tasaki, *Phys. Rev. Lett.* **59**, 799 (1987).
- [30] F. Verstraete and J. I. Cirac, *Phys. Rev. B* **73**, 094423 (2006).
- [31] U. Schollwöck, *Rev. Mod. Phys.* **77**, 259 (2005).
- [32] U. Schollwöck, *Ann. Phys. (Amsterdam)* **326**, 96 (2011).
- [33] C. Hubig, I. P. McCulloch, U. Schollwöck, and F. A. Wolf, *Phys. Rev. B* **91**, 155115 (2015).
- [34] <https://www.calculquebec.ca>.
- [35] <https://www.computecanada.ca>.